

## The Diverse Club: The Integrative Core of Complex Networks

M.A. Bertolero, B.T.T. Yeo, & M. D'Esposito

A complex system can be represented and analyzed as a network, where nodes represent the units of the network and edges represent connections between those units. For example, a brain network represents neurons as nodes and axons between neurons as edges. In many networks, some nodes have a disproportionately high number of edges. These nodes also have many edges between each other, and are referred to as the rich club. In many different networks, the nodes of this club are assumed to support global network integration. However, another set of nodes potentially exhibits a connectivity structure that is more advantageous to global network integration. Here, in a myriad of different biological and man-made networks, we discover the diverse club—a set of nodes that have edges diversely distributed across the network. The diverse club exhibits, to a greater extent than the rich club, properties consistent with an integrative network function—these nodes are more highly interconnected and their edges are more critical for efficient global integration. Moreover, we present a generative evolutionary network model that produces networks with a diverse club but not a rich club, thus demonstrating that these two clubs potentially evolved via distinct selection pressures. Given the variety of different networks that we analyzed—the *C. elegans*, the macaque brain, the human brain, the United States power grid, and global air traffic—the diverse club appears to be ubiquitous in complex networks. These results warrant the distinction and analysis of two critical clubs of nodes in all complex systems.

---

Many complex systems—neural, the power grid, and air traffic—can be analyzed as a network with graph theory, where units (e.g., neurons or airports) and connections (e.g., axons or flight routes) are treated as nodes and edges in a graph, respectively. These systems all exhibit a *community* structure—nodes cluster into communities such that nodes are more strongly connected to other members of their community than to members of other communities<sup>1–4</sup>. Each node within one of these communities can play a distinct role in the overall network topology. In many different systems, from brains to air traffic, applying two nodal role metrics—degree and participation coefficient—to the graph representing the system identifies nodes that have been proposed to be hubs that perform integrative or coordinative functions<sup>5–18</sup>.

Degree is a nodal metric of how many edges the node has. While a node's degree captures its magnitude of connectivity, it does not capture the diversity of the node's connectivity across communities in the network. The participation coefficient is a nodal metric of the *diversity* of each node's connections across the network's communities<sup>10,18</sup>. A node's participation coefficient is maximal if it has an equal number of edges to each community in the network. Mathematically, a node's participation coefficient is independent of the node's degree, as it only measures the diversity of a node's connections across communities. Empirically, across a wide range of networks, the participation coefficient is not correlated with degree, but nodes can be high in both degree and participation coefficient<sup>6</sup>.

Across various networks, nodes with a high degree are connected to each other at a rate greater than would be expected in a randomly organized graph<sup>19</sup>. This subset of highly interconnected nodes is referred to as the “rich club”. The rich club is thought to be critical for global communication given that these nodes have a high betweenness centrality, in that, if the shortest paths between all pairs of nodes is found, many of these shortest paths involve rich club members<sup>20</sup>. Evidencing the rich club's criticality, these brain regions are more likely to exhibit brain pathology than other brain regions in

many neurological and psychiatric disorders<sup>13</sup>. In line with this empirical finding, in silico “attacks” on networks demonstrate that, when edges between nodes in the rich club are removed, global efficiency is decreased (i.e., the sum of shortest paths between all nodes increases)<sup>5</sup>. Given these characteristics, the rich club, which has been investigated in over 200 published reports to date, has been proposed to be an integrative and stable core of brain regions that coordinates the transmission of information across the network.

However, as opposed to the high magnitude of connectivity that high degree nodes exhibit, nodes with a high participation coefficient exhibit diverse connectivity. This connectivity pattern places these nodes at the topological center of the network<sup>21</sup>, ideal for integration and coordination. In the human brain, these nodes are also located where many communities are within close physical proximity<sup>6</sup>, and appear to control or coordinate which regions are “functionally” connected during cognition, in that activity in these nodes predicts changes in the connectivity of other nodes<sup>22,23</sup>, particularly the connectivity between nodes in different communities during cognitive tasks<sup>24</sup>. These nodes have also been implicated in a diverse range of tasks<sup>25,26</sup>. Moreover, damage to these brain regions causes a decrease in the modular architecture of the human brain network<sup>27</sup> and widespread cognitive deficits<sup>28</sup>. Finally, a recent analysis showed that only these brain regions exhibit increased activity if more communities are engaged in a cognitive task, which suggests that they are involved in processes that are more demanding as more communities are engaged<sup>2</sup>. A parsimonious explanation of these empirical findings is that nodes with high participation coefficients integrate information and coordinate connectivity between communities, which allows for modular local processing.

Thus, nodes with both a high participation coefficient and a high degree have been proposed to perform integrative and coordinative functions. Here, we make a comprehensive distinction between high degree and high participation coefficient nodes. We demonstrate, with data from multiple systems, that networks contain a *diverse club*—a set of high participation coefficient nodes that are more highly interconnected than the rich club. We find that the two clubs are largely comprised of different nodes. Moreover, we analyze the anatomical locations of these clubs in the human brain, the connectivity patterns of these clubs, the functional responses of both clubs in the human brain during cognitive tasks, and how damage to nodes in each club impacts the network’s efficiency. Finally, we present a generative evolutionary network model that generates graphs with a diverse club but not a rich club. From these analyses, we demonstrate that the diverse club exhibits, to a greater extent than the rich club, properties that are consistent with an integrative and coordinative function. Together, these results support the distinct roles of the diverse club and rich club in network communication.

## Clubness

We analyzed structural and functional networks from multiple species—the *c. elegans*’ structural and functional networks, the macaque structural network, the human functional network, the United States power grid network, and the global air traffic network (see Methods for network construction details). We consider both structural and functional networks, as degree can be artificially inflated in functional (i.e., correlational) networks<sup>6</sup>. Graph theory allows for the comparison of network organization among very different systems. While the *c. elegans* networks, the macaque network, and the human brain networks are clearly different networks, they are all biological neural networks that were shaped by evolution. Thus, we also investigated man-made networks to determine if they exhibit properties similar to the biological networks.

The rich club is the set of high degree nodes in a graph; it is referred to as a club because these nodes are highly interconnected to each other. We refer to how interconnected a club is as “clubness”. We measure clubness with the normalized club coefficient, which is the number of intra-club edges the club has relative to the mean of that value in a large set (here, 1000) of random graphs. These random graphs are generated based on the original graph; all nodes maintain their degree, but the edges are randomly placed and the edge weights (in the *C. elegans* functional networks, human functional networks, and air traffic network; other networks contain only binary edges) are shuffled between nodes with the same degree, which accounts for the contribution of both edge placement and edge weight to the normalized club coefficient<sup>19</sup>. Results were very similar without shuffling edge weights, which only accounts for the contribution of edge placement (Extended Data Figures 1, 2).

For every network, we defined the rich club and its clubness across different ranks. A rank defines the cutoff for which nodes are in the rich club. For example, in a network with 100 nodes, a rank of 85 contains nodes with a degree greater than or equal to the value of the node with the 15<sup>th</sup> highest degree. Here, weighted degree (sum of edge weights) was used if the network was weighted. In addition, for every network, we defined the diverse club—the club of high participation coefficient nodes—and its clubness at each rank. We then used a myriad of analyses to characterize, and make distinctions between, the rich club (i.e. high degree nodes) and the diverse club (i.e. high participation coefficient nodes) in each network.

### **Clubness of the rich club and the diverse club**

We sought to measure if the diverse club or the rich club is more interconnected than the other. For each network, we applied community detection using InfoMap<sup>29</sup> (e.g., Extended Data Figure 3). Next, we calculated the degree and participation coefficient of each node in every network. Using these values, for each network, we calculated the clubness for both clubs at every possible rank. For both clubs, for every network, as the rank increased, clubs with a clubness greater than 1 (i.e., 1 means equal to random) were detected (Figure 1, Extended Data Figures 1, 2, and 4). However, in every network, as the rank increased to only include those nodes with the highest degree or participation coefficient, the clubness of the diverse club was higher than that of the rich club. These results demonstrate that, across a range of networks, the club of high participation coefficient nodes (the diverse club) is more strongly interconnected than the club of high degree nodes (the rich club).

### **Network topology of the rich club and the diverse club**

We further analyzed clubs at the rank that corresponds to the 80<sup>th</sup> percentile, as this is the rank, across networks, where the normalized club coefficient increased dramatically. For example, in the human brain networks, which contain 264 nodes, the clubs contained 53 nodes each. To visualize the spatial topology of the derived network communities, we used the ForceAtlas2<sup>30</sup> algorithm, which simulates a physical system in which nodes repel each other like charged particles and edges attract their nodes like springs, which results in nodes in the same community pulling together, and different communities pulling apart from one another. We labeled each node in the graph by their community affiliation and their membership in a rich or diverse club (Figure 2 shows the communities in *C. elegans* and human resting-state; Extended Data Figure 3 shows a non-biological network, e.g. air traffic).

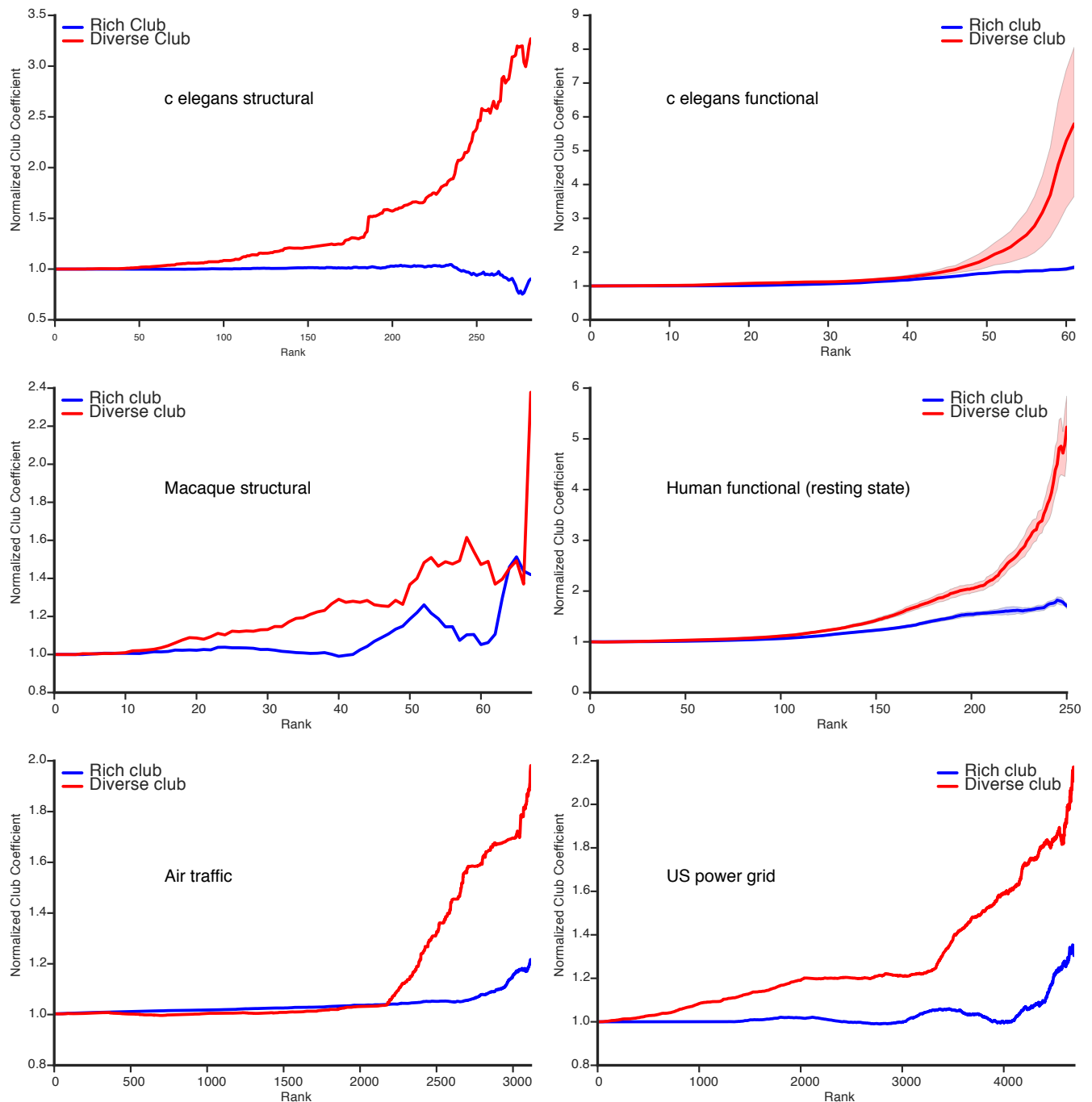


**Figure 1 | Clubness of the diverse and rich clubs.** Normalized club coefficients (clubness) for the rich and diverse clubs in every network. For functional networks, the mean across network costs for the clubness is plotted, with 95 percent confidence intervals shaded. In every network, as the rank increased and only nodes with a high participation coefficient (red) or degree (blue) are included in the club, the diverse club is consistently higher in clubness than that of the rich club.

Visual inspection of the c. elegans and human functional networks (Figure 2a,b) suggests that rich club nodes exist on periphery of the graph, whereas diverse club nodes are in the center. There are few nodes that are members of both clubs. Anatomically in the human brain resting-state network, the rich club and diverse club are differentially represented in different communities (Figure 2c,d). These analyses demonstrate that the clubs exist at different anatomical locations in the human brain as well as different topological locations in the graph.

We then quantified how similar the clubs are in each network, measuring the percentage of possible overlap. Zero percent represents that no nodes were members of both clubs, and 100 percent represents that the clubs are identical. In the human networks, across both resting-state and 6 task states, no more than 11 percent of nodes were in both clubs (Figure 3a). In the functional *c. elegans* networks, the overlap ranged from 11 to 35 percent (Extended Data Figure 5). The structural networks from *c. elegans* and macaque, and the air traffic and US power grid networks, showed the highest overlap, ranging from 37 to 50 percent (Extended Data Figure 5). These analyses demonstrate that the diverse and rich clubs are predominately comprised of different nodes.

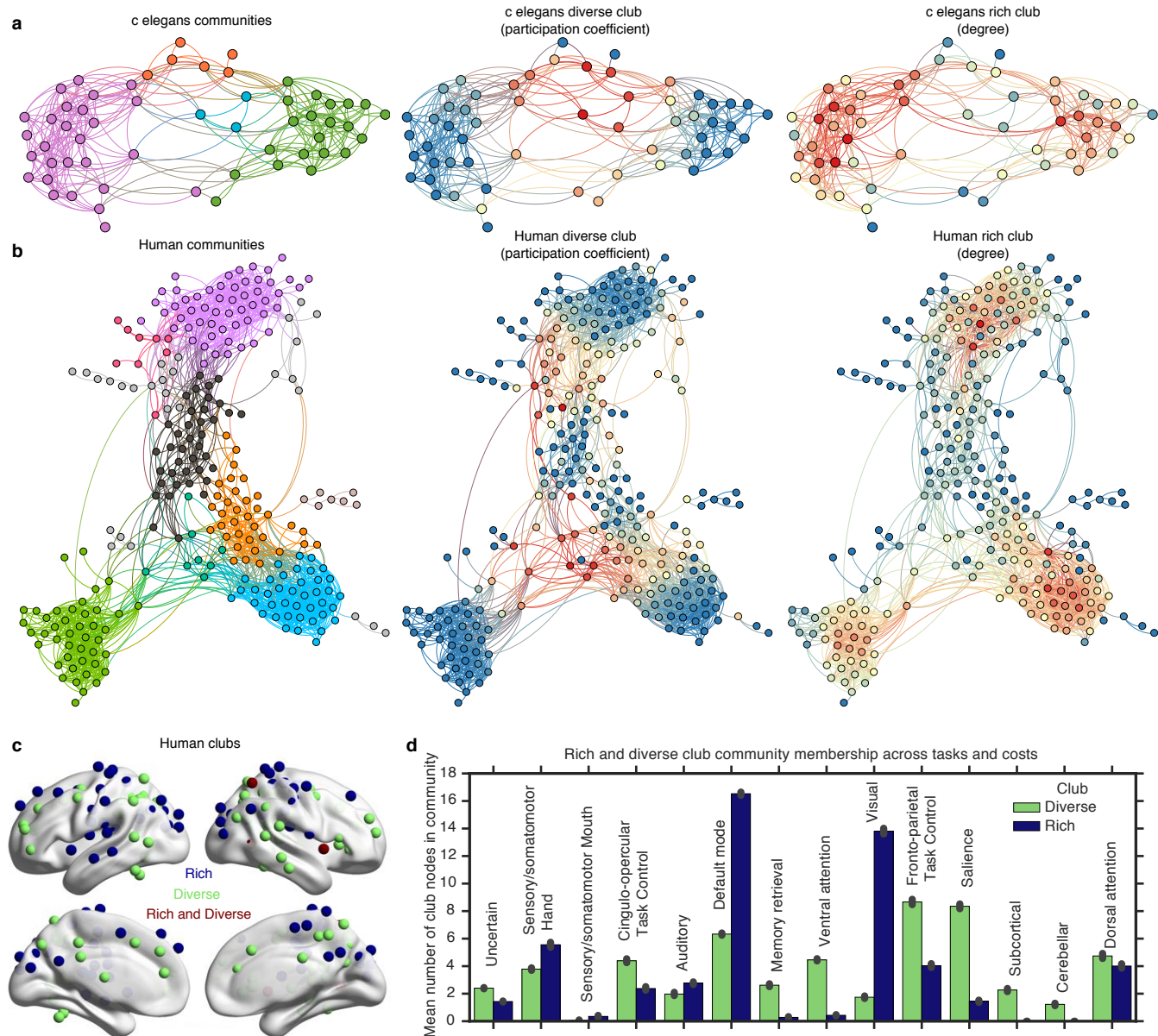


**Figure 2 | Topology of the diverse and rich clubs.** **a**, Visualization of a single *c. elegans* functional network, labeled according to the community affiliation, the diverse club, and the rich club. Nodes in red represent the maximum value for the given metric, yellow is median, and blue is the minimum. Edges are colored by the mix between the two nodes each edge connects. **b**, Visualization of the human resting-state network labeled according to the community affiliation, the diverse club, and the rich club. In both networks, the diverse club clusters in the center of the layout, while the rich club forms clusters on the periphery. **c**, The rich club and the diverse club (human resting-state), along with nodes that are members of both clubs, are shown on the cortical surface of the human brain. **d**, The mean number of club nodes (across costs and tasks) in each functional community identified in the human fMRI data. Community names and division from a previous publication<sup>3</sup>.

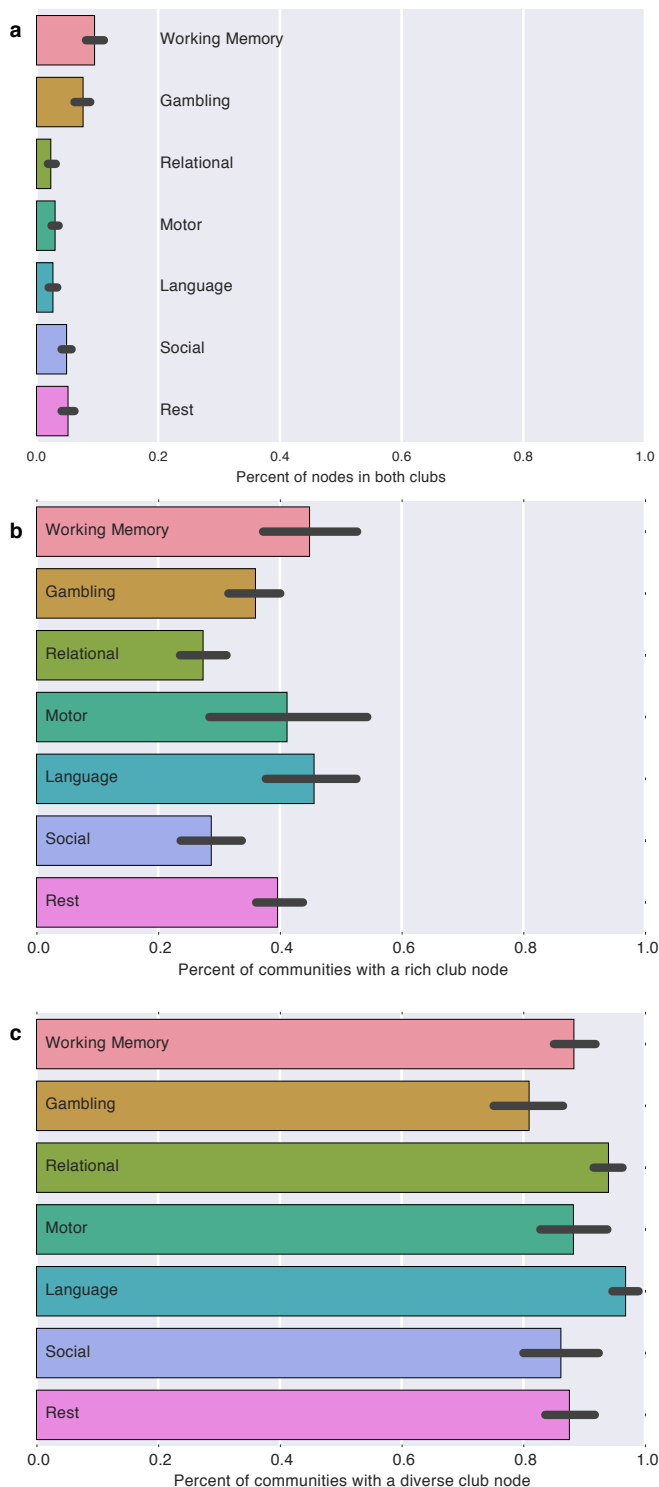


**Figure 3 | Distribution of nodes in clubs and communities.** **a**, The percentage of nodes in human functional networks that are in both the rich and diverse clubs. Zero percent represents that no nodes were members of both clubs, and 100 percent represents that the clubs are identical. No larger than 11 percent overlap was found across costs (0.05-0.20) and networks. The percentage of communities that contain a node from the rich club (**b**) or the diverse club (**c**). 100 percent represents that every community contains at least one node from that club.

Given that the diverse club appears to be in the topological center of complex networks, and an integrative club of nodes should have members in many different communities, we tested how many communities has a member of each club. Across all networks, a higher percentage of communities contained a node in the diverse club than the rich club (Figure 3b,c, Extended Data Figure 6).

We next tested if the betweenness centrality—the number of shortest paths between pairs of nodes that pass through a node—of the diverse club is higher than that of the rich club. Across all networks we analyzed, the betweenness centrality of the diverse club was either significantly higher than the rich club or there was no significant difference (Extended Data Figure 7). Betweenness centrality, however, does not capture if the network’s shortest paths traverse edges between nodes in the rich or diverse club. Thus, we measured the edge betweenness—how many shortest paths between pairs of nodes traverse a particular edge—of the edges between members of the rich club or the diverse club. With this calculation, in almost all networks, the edge betweenness was significantly higher for the diverse club than the rich club. It was not significantly higher in the structural *c. elegans* and macaque networks (Extended Data Figure 7). Moreover, in the air traffic network, until the clubs reached a size of 356 airports (approximately 10 percent of all airports), the diverse club had more international airports in it than the rich club. Furthermore, flights between airports not in the diverse club are predominately domestic, while international flights were mainly between diverse club airports; this was not the case for the rich club and non-rich club airports (Extended Data Figure 3). These analyses demonstrate that, relative to the rich club, the diverse club is represented in more communities and more shortest paths between nodes pass through the diverse club. These are two properties that are likely critical for global network integration and communication.

### Diverse and rich club activity during cognitive tasks

Previously, using the BrainMap database, we demonstrated that the diverse club (nodes with a high participation coefficient) exhibits increased activity in

tasks that engaged more cognitive components or communities (see <sup>2,26</sup> for detailed descriptions). Using the Human Connectome Database resting-state network studied here, we replicated these findings—increased activity of the diverse club was correlated with the number of cognitive components ( $r=0.41$ ,  $p=0.0002$ ) and communities ( $r=0.40$ ,  $p=0.0003$ ) a task engaged. For the rich club, nodes exhibited significantly decreased activity as more cognitive components ( $r=-0.53$ ,  $p=1e-7$ ) or communities were engaged in a task ( $r=-0.33$ ,  $p=0.003$ ). Thus, the diverse club, not the rich club, exhibits increased activity when more communities are engaged in a task, which likely occurs when more integration across and coordination between communities is required.

### **Targeted attacks of intra-club connections**

To further investigate the importance of the diverse and rich clubs for efficient global communication in a network, we simulated lesioning intra-club connections. For each network, in 10,000 iterations, we removed between (randomly) 50 and 90 percent of edges from either club (skipping edges that disconnected the graph into two sub-graphs). We then calculated the increase in the sum of shortest paths, which indicates decreased global efficiency. In every network, removing edges between diverse club nodes increased the sum of shortest paths to a greater extent than removing edges between rich club nodes (Extended Data Figure 8). This demonstrates that the edges in the diverse club, rather than the rich club, are more critical to efficient global communication.

### **A generative model of the diverse club**

Evolutionary pressures have selected networks with rich clubs and diverse clubs. Thus, the final distinction between the diverse club and the rich club we sought to make is if these clubs were potentially naturally selected for different reasons. One of the first observations in neuroscience—Cajal’s conservation principle—was that the brain is organized by an economic trade-off between minimizing the number of connections in the network and adaptive topological patterns<sup>31</sup>. One topological pattern that might be adaptive is modularity, which is how sparse the connectivity is between communities relative to the connectivity within communities. Another potentially adaptive topological pattern is efficiency, which is the inverse of the sum of shortest paths between all nodes, and thus measures how efficiently signals can be integrated across the network. For example, in brain networks, efficiency is used as a measure of the overall capacity for parallel information transfer and integrated processing<sup>21</sup>. Networks that are modular (i.e., exhibit high clustering) and efficient are described as “small world”<sup>32</sup>. Thus, we asked the question: do evolutionary pressures that select high modularity and efficiency given a limited number of connections generate a network topology that contains a rich club or a diverse club? In other words, is one of the clubs nature’s solution to efficient integrative processing in a modular network?

To answer this question, we developed a generative graph model that maximizes  $Q$  and efficiency. The model starts with a graph of 100 nodes that are randomly connected, with 5 percent of all possible edges (272 binary edges). To simulate natural selection of high  $Q$  and efficiency, we found edges that, when removed, increase  $Q$  and decrease efficiency the least. We remove these edges and then randomly place them back in the network, thus artificially selecting edges in the graph that maximize  $Q$  and efficiency. We also ran the same model, except we randomly selected the edges, removed them, and then randomly placed them in the network. This allowed us to decipher if the model selects a network with a diverse club that is more highly interconnected than if random selection had occurred. Our hypothesis was that, if the diverse club is nature’s solution to efficient integrative processing in a modular network, a highly interconnected diverse club, but not a rich club, will emerge when networks are selected based on maximizing modularity and efficient integration.



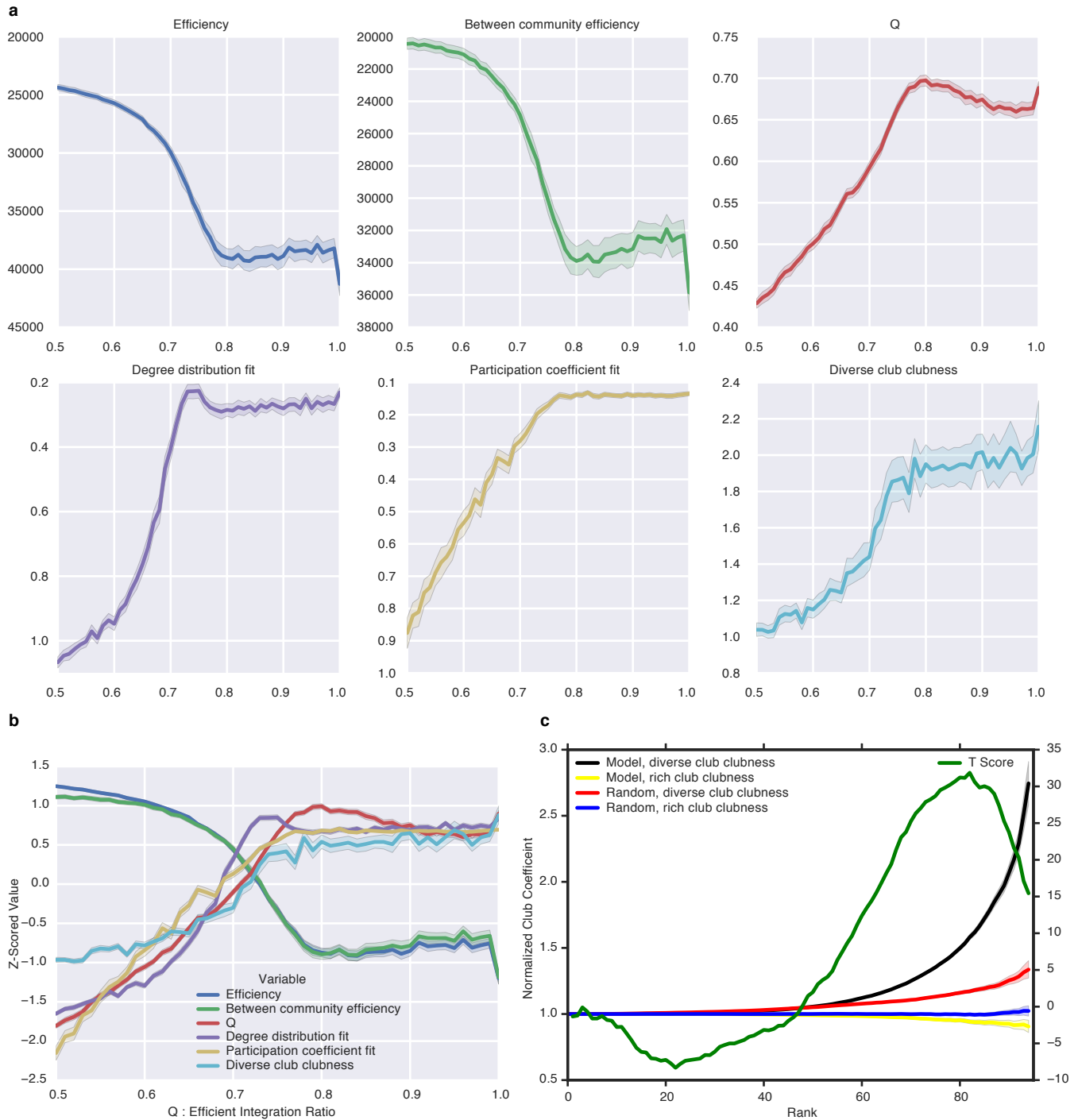


**Figure 4 | A generative model of the diverse club.** **a**, Six features of the network were analyzed across different ratios of maximizing Q and efficiency (inverse of the sum of shortest paths between all nodes). 100 models were run at each ratio in 0.01 steps. Each value's mean and 95 percent confidence intervals (shaded) are shown. **b**, At ratios of 0.7 to 0.8 between weighting modularity and weighting efficiency, a balance between these six variables was achieved. **c**, The average clubness across 1000 iterations for each rank for the diverse and rich clubs in the generative model at a ratio of 0.75 and the random model, as well as the t-test at each rank between the clubness of the diverse club in the model and the random model (similar results from ratios of 0.70 and 0.80 are shown in Extended Data Figure 9). Only the diverse club in the model has a high normalized club coefficient.

We varied the amount of importance Q or efficiency played in the selection of edges. A ratio of 0.5 equally maximized both Q and efficiency, while 1 maximized only Q. We found that, at a ratio of 0.75 (Q) to 0.25 (efficiency), a balance was achieved with high efficiency, high between community efficiency (the inverse of the sum of shortest paths between nodes in different communities), high modularity, a high correspondence between the degree distribution of the model network and the



human brain network (resting-state), a high correspondence between the participation coefficient distribution of the model network and the human brain network (resting-state), and a high clubness of the diverse club. Figure 4 shows these values individually (a) and together (b) across different ratios of maximizing Q versus efficiency.

Using a ratio of 0.75, we ran 1000 iterations of the model and 1000 iterations of the random model. We then calculated the clubness of the diverse club in the model and the random model. We found that, at higher ranks, the clubness of the diverse club in the models that maximize Q and efficiency was higher than the clubness of the diverse club in the random models (Figure 4c; ratios of 0.70 and 0.8 led to similar results (Extended Data Figure 9)). This demonstrates that the diverse club's high clubness is not a mathematical necessity of defining the club based on high participation coefficients, as randomly selected networks do not exhibit a highly interconnected diverse club. Thus, the diverse club's strong interconnectedness is a non-trivial feature of real networks. Moreover, we did not find high clubness of the rich club in the model. Thus, while the diverse club was captured by the generative model, the rich club was not captured by this model. These results suggest that the diverse club, but not the rich club, might be nature's solution to efficient integrative processing in a modular network.

## Discussion

Nodes in a network with many edges (i.e. high degree nodes) or with edges that are diversely distributed across communities (i.e. high participation coefficient nodes) have both been suggested to be integrative hubs<sup>5–18</sup>. Here, we provided evidence that high participation coefficient nodes, which we refer to as the diverse club, have properties that are more characteristic of integrative hubs, as compared to high degree nodes (i.e., the rich club). The diverse club is more interconnected than the rich club in every network we analyzed—the human brain (in 7 different states), the *C. elegans*, the macaque brain, the United States power grid, and global air traffic. In the human brain, diverse club nodes are up to four times as interconnected as rich club nodes. Importantly, in all networks examined—especially in the functional brain networks, *C. elegans* structural network, and the man-made networks—very few nodes are members of both clubs.

Having established that the diverse club is relatively distinct from the rich club, we further differentiated the functions of these two clubs in a myriad of analyses. The diverse club spans more communities and has higher edge betweenness and betweenness centrality than the rich club. This pattern of connectivity, which is spread across the entire network and exhibits the most economical route between nodes, is a critical property of nodes that integrate across network communities. Moreover, in humans, these two clubs exhibit different activity patterns as cognitive tasks become more complex. Unlike rich club nodes, diverse club nodes increase activity in response to more communities being engaged by a task, which likely requires more integration across the network's communities. Finally, across all networks, edges between diverse club nodes are more critical to efficient global communication than the edges between rich club nodes. When diverse club edges were removed, the sum of shortest paths between nodes increased significantly more than when rich club edges were removed.

We also investigated if the two clubs might have distinct evolutionary origins. Many of the brain's network properties that are related to integration are heritable and impact its fitness—how likely that brain network architecture is to be naturally selected. Specifically, the brain network's cost-efficiency ratio (high efficiency given a constrained number of connections—the *wiring cost*) is heritable. Moreover, the diverse club's local efficiency (the sum of each node's shortest paths to all nodes) is

heritable<sup>33</sup>. Efficiency is also behaviorally relevant, making it likely to factor in natural selection. For example, working memory performance is correlated with network efficiency, and individuals with schizophrenia have lower efficiency and working memory performance<sup>34</sup>. Also, higher intelligence quotient scores are associated with higher network efficiency and betweenness centrality of the fronto-parietal network (which we found to have the highest number of diverse club nodes)<sup>35–37</sup>. However, brain networks are not purely optimized for efficiency, given that they exhibit high modularity, with segregated communities performing distinct functions, at the cost of lower efficiency<sup>38–40</sup>. Modularity likely increases fitness in information processing systems<sup>41–43</sup> and confers robustness to network dynamics (i.e., information processing) when the connections between nodes are reconfigured, a process necessary for the evolution of a network<sup>44</sup>. Modular networks also outperform and evolve faster than non-modular networks<sup>45</sup> with lower wiring costs than non-modular networks<sup>46</sup>. Like efficiency, modularity is also behaviorally relevant, and thus potentially naturally selectable. For example, modularity explains intra-individual variation in working memory capacity<sup>47</sup> and predicts how well an individual will respond to cognitive training<sup>48</sup>.

As modularity and efficiency are both heritable and impact the fitness of an organism, we probed the possible evolutionary origins of the two clubs by asking if the rich or diverse club was selected to balance efficient global integration without sacrificing modularity. We found that, if we simulate natural selection for a balance between modularity and efficient integration, a highly interconnected diverse club, but not a rich club, emerges. Thus, the diverse club potentially evolved via selective pressures that favored both modularity and efficient integration. This provides further evidence for dissociable functions of these clubs. Additionally, the evolutionary generative model, compared to the random null model, produced significantly higher clubness in the diverse club. This demonstrates that the high clubness of the diverse club is only a feature of real world networks with a non-random architecture.

The interpretation of many previous network analyses could be dramatically altered in light of our findings, as our results provide a strong motivation for the consideration of both a rich and diverse club in network function. Contrary to previous proposals, we propose that the true integrative core of networks is the diverse club, not the rich club. Thus, we hypothesize that the rich club likely plays an alternative role in network function. One possibility that has been previously suggested is that the rich club maintains the stability of the dynamics of spontaneous activity. In the macaque structural network, rich club nodes exhibit very high in-degree—many white matter connections terminate on these nodes. Thus, autonomous dynamics of the rich club are largely constrained by the summary of strong rhythmic outputs from the entire network—rich club nodes stay closer to the summated and global network oscillations than other nodes and thus promote stability in the network dynamics at slower time-scales<sup>49</sup>. An analogy can be made in social networks where members that exhibit a high in-degree, like politicians, are “slaves to their own power”, as they are only able to act in limited, and often slow, ways that mostly reflect the entire social network<sup>49</sup>.

The functional connectivity, anatomical location, and cognitive functions of rich club nodes in humans fit with this proposal. The default-mode network (which we found has the highest concentration of rich club nodes), is equidistant and maximally distant from primary sensory and motor networks based on both functional connectivity and anatomical geodesic distance<sup>50</sup>. Moreover, a meta-analysis of human brain imaging data showed that the default mode network is involved in tasks unrelated to immediate stimulus input, such as daydreaming or mind-wandering<sup>50</sup>. These empirical findings suggest that the function of the rich club may predominately be to maintain stability in the entire network via slow processing, potentially using its high degree to integrate information at slower time scales, in contrast to the diverse club, which may act on shorter time scales. This potential distinction between the rich and diverse club warrants further investigation.

## Methods

**c. elegans network data.** Four *c. elegans* worms were imaged while executing behavior with calcium imaging, and each neuron's extracted time series of activity was made publically available<sup>51</sup>. In this analysis, each neuron was treated as a node, and the edge weights between nodes  $i$  and  $j$  represented the Pearson  $r$  correlation (no Fisher transform was applied, as the original paper analyzed raw  $r$  values and  $r$  values were not averaged across worms) between the time series of nodes  $i$  and  $j$ . The worms had 56, 77, 68, and 57 nodes. Each worms' graph was thresholded at a particular cost, retaining 5 to 20 percent of possible edges in 1 percent intervals. The maximum spanning tree (the set of edges (i.e., path) that connects all nodes with the maximum sum of edge weights possible) for each graph was calculated, and these edges were not removed in order to keep the graph connected. Community detection was applied at every cost separately, using the InfoMap algorithm. We also analyzed the structural network of the *c. elegans*<sup>52</sup>, where we constructed a binary and undirected network of all 297 neurons and their 2359 axonal connections (i.e., no thresholding).

**Human functional MRI (fMRI) data.** Human fMRI data from 471 subjects (S500 release) during rest and the performance of six tasks from the Human Connectome Project<sup>53</sup> were used. For the task fMRI data, Analysis of Functional Neuroimages (AFNI)<sup>54</sup> was used to preprocess the images, matching traditional resting-state functional connectivity studies. The AFNI command *3dTproject* was used, passing the mean signal from the cerebral spinal fluid mask, the mean signal from the white matter mask, the mean whole brain signal, and the motion parameters to the “-ort” options, which remove the signals via linear regression. The options “-automask”, which generates the mask automatically was used. The “-passband 0.009 0.08” option, which removes frequencies outside 0.009 and 0.08, was used. Finally, the “-blur 6”, was used, which smooths the images inside the mask only) with a filter that has a width (FWHM) of 6mm after the time series filtering. We analyzed the working memory (405 timepoints), relational reasoning (232 timepoints), motor (284), social cognition (274 timepoints), mixed math and language (316), and gambling tasks (253 timepoints). Given the short length (176 timepoints, and thus low degrees of freedom during preprocessing) of the Emotion task, it was not included in our analyses. For the resting state fMRI data (1200 timepoints), we used the images that were previously preprocessed with ICA-FIX. The AFNI command *3dBandpass* was used to further preprocess these images. We used it to remove the mean whole brain signal and frequencies outside 0.009 and 0.08 (explicitly, “-ort whole\_brain\_signal.1D -band 0.009 0.08 -automask”).

For each task (both LR and RL encoding directions were used), for each subject, the mean signal from 264 regions in the Power atlas<sup>3</sup> was computed. The Pearson  $r$  between all pairs of signals was computed to form a 264 by 264 matrix, which was then Fisher  $z$  transformed. All subjects' matrices were then averaged. No negative correlations were included in our analyses. This matrix served as the edge weights for the graph for that particular task. The same thresholding and analyses across costs that was applied to the *c. elegans* functional networks was executed for human networks.

**Macaque structural network.** The structural network of the macaque cortex is publically available<sup>55</sup>. While the *c. elegans* is a micro-scale network, with individual neurons represented as nodes, the macaque network is a macro-level network, with 71 brain regions modeled as nodes and 438 white matter tracts modeled as edges. Edges were treated as undirected and binary; thus, no thresholding and analyses across costs is required.

**Man-made networks.** We analyzed air traffic patterns between 3281 airports and 531 airlines spanning the globe, where a node is an airport, and the edge weight between nodes is the number of airlines flying between them, resulting in 10,924 edges (data downloaded from OpenFlights.org). We also analyzed the United States power grid, where a node is either a generator, a transformer, or a substation (n=4,941), and an edge represents a power supply line (n=6,594). No thresholding was applied to either network. Data was downloaded from: <http://konect.uni-koblenz.de/networks/opsahl-powergrid>.

**Generative evolutionary model.** The model starts with a graph of 100 nodes that are randomly connected, with 5 percent of all possible edges (n=272). Binary edges were used. At each iteration, the change in Q and the change in the sum of shortest paths following the removal of each edge is calculated. Edges are chosen for removal that, when removed, lead to a maximal increase in Q and a minimal increase in the sum of shortest paths. These edges are removed and then randomly placed back in the graph, maintaining a constant density of edges (0.05). At each iteration, 0.25 percent of edges are removed from the graph and then placed randomly back into the network. This process maximizes Q and minimizes the sum of shortest paths. This procedure is repeated for 150 iterations, resulting in 1950 edges being shuffled. At this point, the generative model stops. For a null model, we also ran the generative process, except we randomly selected the edges, removed them, and then randomly placed them in the network.

The degree and participation coefficient fit was measured by the inverse of Kullback-Leibler divergence:  $\sum(pk \cdot \log(pk / qk), \text{axis}=0)$ , where  $pk$  is histogram of the model network's distribution and  $qk$  is the histogram of the human brain network's distribution, both of which have been sorted into 10 bins, where each bin's value is the proportion of nodes in that bin. This was implemented in python as `scipy.stats.entropy(model_histogram,human_brain_histogram)`.

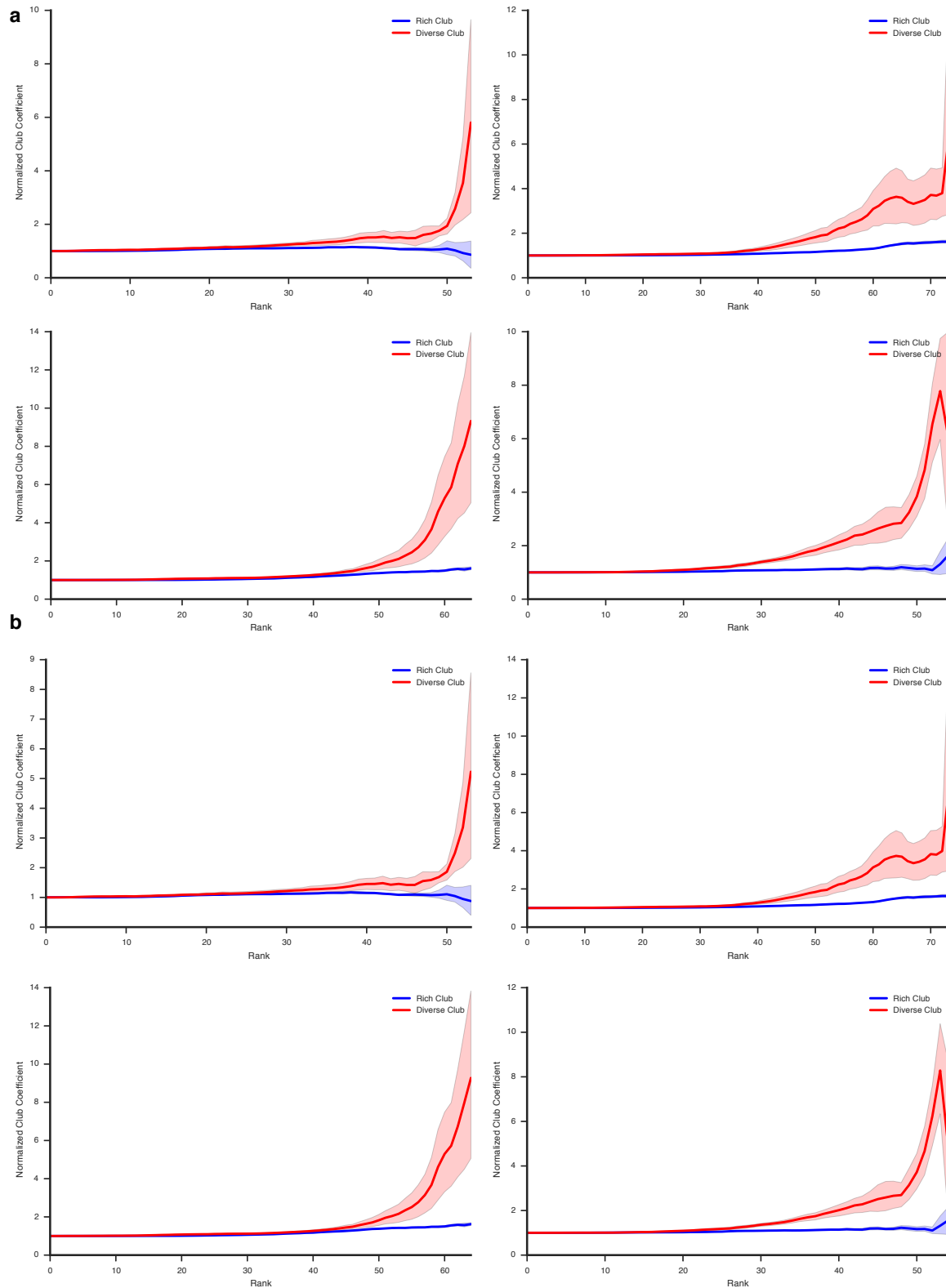
## References

1. Yeo, T. *et al.* The organization of the human cerebral cortex estimated by intrinsic functional connectivity. *J Neurophysiol* **106**, 1125–1165 (2011).
2. Bertolero, M. A., Yeo, T. B. & D'Esposito, M. The modular and integrative functional architecture of the human brain. *Proceedings of the National Academy of Sciences* **112**, 201510619–E6807
3. Power, J. *et al.* Functional Network Organization of the Human Brain. *Neuron* **72**, 665–78 (2011).
4. Newman, MEJ. Modularity and Community Structure in Networks. *Proceedings of the National Academy of Sciences of the United States of America* **103**, 8577–8582
5. Van den Heuvel, MP & Sporns, O. Rich-Club Organization of the Human Connectome. *Journal of Neuroscience* **31**, 15775–15786
6. Power, J., Schlaggar, B., Lessov-Schlaggar, C. & Petersen, S. Evidence for Hubs in Human Functional Brain Networks. *Neuron* **79**, 798–813 (2013).
7. Schmidt, R., LaFleur, K., de Reus, M., van den Berg, L. & van den Heuvel, M. Kuramoto model simulation of neural hubs and dynamic synchrony in the human cerebral connectome. *BMC neuroscience* **16**, 54 (2015).
8. Liska, A., Galbusera, A., Schwarz, A. J. & Gozzi, A. Functional connectivity hubs of the mouse brain. *NeuroImage* **115**,
9. Scholtens, L. H., Schmidt, R., de Reus, M. A. & van den Heuvel, M. P. Linking macroscale graph analytical organization to microscale neuroarchitectonics in the macaque connectome. *The Journal of neuroscience : the official journal of the Society for Neuroscience* **34**, 12192–12205
10. Guimera, R., Mossa, S., Turttschi, A & Amaral, LAN. The worldwide air transportation network: Anomalous centrality, community structure, and cities' global roles. *Proceedings of the National Academy of Sciences* **102**, 7794–7799

11. Towlson, EK, Vertes, PE, Ahnert, SE, Schafer, WR & Bullmore, ET. The Rich Club of the C. elegans Neuronal Connectome. *Journal of Neuroscience* **33**, 6380–6387
12. Grayson, D. *et al.* Structural and Functional Rich Club Organization of the Brain in Children and Adults. *PLoS ONE* **9**, e88297 (2014).
13. Crossley, NA *et al.* The hubs of the human connectome are generally implicated in the anatomy of brain disorders. *Brain : a journal of neurology* **137**, 2382–2395
14. Guimera, R, Sales-Pardo, M & Núñez-Amaral, LA. Classes of complex networks defined by role-to-role connectivity profiles. *Nature Phys.* **3**, 63–69
15. Bacik, K., Schaub, M., Beguerisse-Díaz, M., Billeh, Y. & Barahona, M. Flow-Based Network Analysis of the Caenorhabditis elegans Connectome. *PLOS Computational Biology* **12**, e1005055 (2016).
16. Sporns, O., Honey, C. & Kötter, R. Identification and classification of hubs in brain networks. *PloS one* **2**, e1049 (2007).
17. Van den Heuvel, MP & Sporns, O. An Anatomical Substrate for Integration among Functional Networks in Human Cortex. *Journal of Neuroscience* **33**, 14489–14500
18. Guimerà, R. & Amaral, L. Functional cartography of complex metabolic networks. *Nature* **433**, 895–900 (2005).
19. Alstott, J., Panzarasa, P., Rubinov, M., Bullmore, E. & Vértés, P. A unifying framework for measuring weighted rich clubs. *Scientific reports* **4**, 7258 (2014).
20. De Reus, M. & van den Heuvel, M. Rich Club Organization and Intermodule Communication in the Cat Connectome. *The Journal of Neuroscience* **33**, 12929–12939 (2013).
21. Bullmore, E. & Sporns, O. The economy of brain network organization. *Nature Publishing Group* 1–14 doi:10.1038/nrn3214
22. Bassett, D. S., Yang, M., Wymbs, N. F. & Grafton, S. T. Learning-induced autonomy of sensorimotor systems. *Nature Neuroscience* **18**, 744–751
23. Spadone, S. *et al.* Dynamic reorganization of human resting-state networks during visuospatial attention. *Proceedings of the National Academy of Sciences of the United States of America* **112**, 8112–7 (2015).
24. Gratton, C., Laumann, T., Gordon, E., Adeyemo, B. & Petersen, S. Evidence for Two Independent Factors that Modify Brain Networks to Meet Task Goals. *Cell reports* **17**, 1276–1288 (2016).
25. Cole, M. W. *et al.* Multi-task connectivity reveals flexible hubs for adaptive task control. *Nature Neuroscience* **16**, 1348–1355
26. Yeo, T. *et al.* Functional Specialization and Flexibility in Human Association Cortex. *Cerebral Cortex* **25**, 3654–3672 (2015).
27. Gratton, C., Nomura, E., Pérez, F. & D’Esposito, M. Focal brain lesions to critical locations cause widespread disruption of the modular organization of the brain. *Journal of cognitive neuroscience* **24**, 1275–85 (2012).
28. Warren, D. *et al.* Network measures predict neuropsychological outcome after brain injury. *Proceedings of the National Academy of Sciences* **111**, 14247–14252 (2014).
29. Rosvall, M. & Bergstrom, C. Maps of random walks on complex networks reveal community structure. *Proceedings of the National Academy of Sciences of the United States of America* **105**, 1118–23 (2008).
30. Jacomy, M., Venturini, T., Heymann, S. & Bastian, M. ForceAtlas2, a Continuous Graph Layout Algorithm for Handy Network Visualization Designed for the Gephi Software. *PLoS ONE* **9**, e98679 (2014).
31. Y Cajal, S. & y Cajal, S. Texture of the Nervous System of Man and the Vertebrates. 39–51 (2000). doi:10.1007/978-3-7091-6315-3\_3
32. Bassett, D. & Bullmore, E. Small-world brain networks. *The Neuroscientist* **12**, 512–523
33. Fornito, A. *et al.* Genetic influences on cost-efficient organization of human cortical functional networks. *The Journal of neuroscience : the official journal of the Society for Neuroscience* **31**, 3261–70 (2011).
34. Bassett, D. *et al.* Cognitive fitness of cost-efficient brain functional networks. *Proceedings of the National Academy of Sciences of the United States of America* **106**, 11747–52 (2009).
35. Langer, N. *et al.* Functional brain network efficiency predicts intelligence. *Human brain mapping* **33**, 1393–406 (2012).

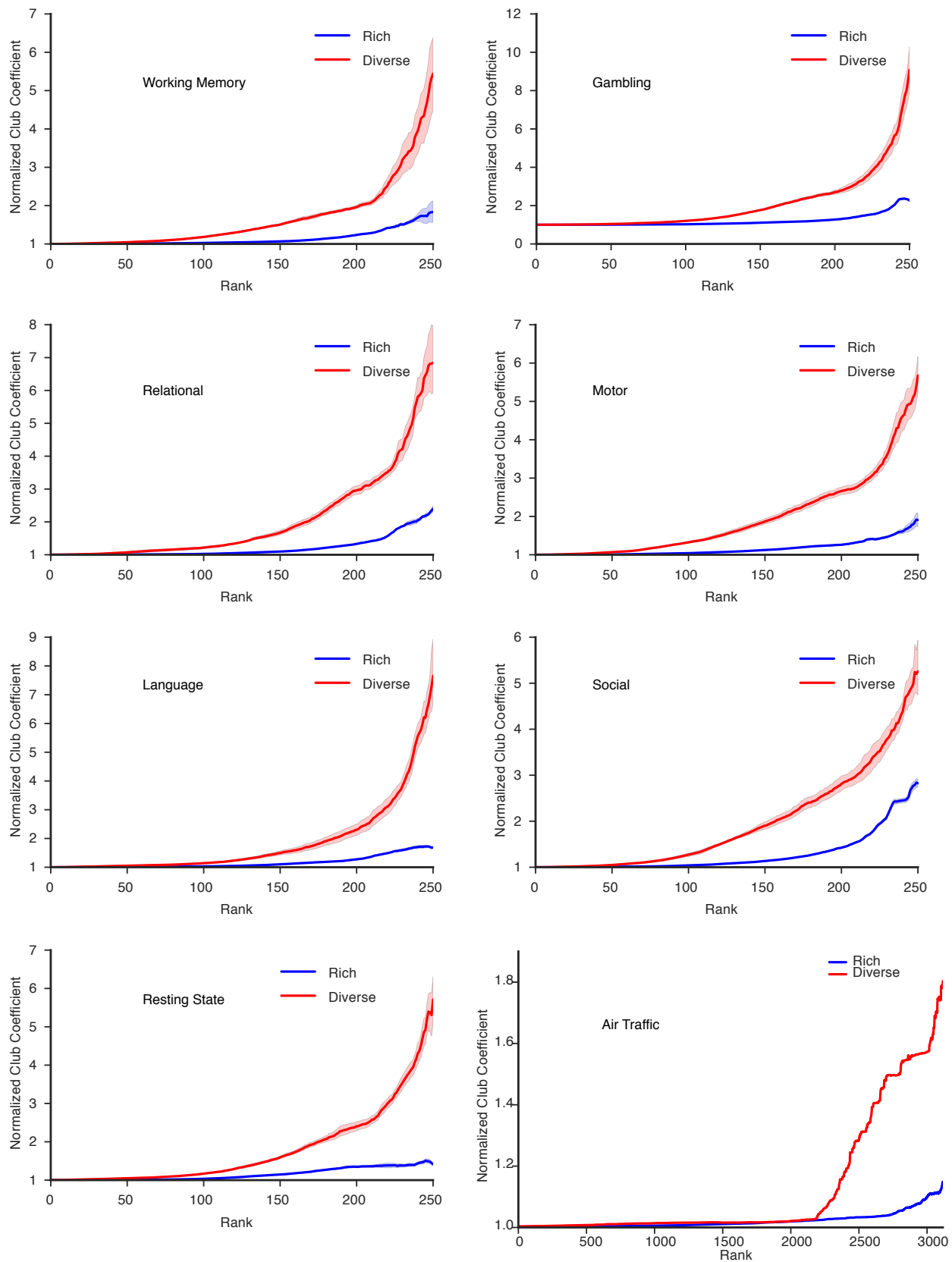
36. Khundrakpam, B. *et al.* Imaging structural covariance in the development of intelligence. *NeuroImage* (2016). doi:10.1016/j.neuroimage.2016.08.041
37. Li, Y. *et al.* Brain anatomical network and intelligence. *PLoS computational biology* **5**, e1000395 (2009).
38. Watts & Strogatz. Collective dynamics of ‘small-world’ networks. *Nature* **393**, 440–2 (1998).
39. Deco, G., Tononi, G., Boly, M. & Kringelbach, M. Rethinking segregation and integration: contributions of whole-brain modelling. *Nature reviews. Neuroscience* **16**, 430–9 (2015).
40. Zamora-López, G., Chen, Y., Deco, G., Kringelbach, M. & Zhou, C. Functional complexity emerging from anatomical constraints in the brain: the significance of network modularity and rich-clubs. *Scientific reports* **6**, 38424 (2016).
41. Klir, G. & Simon, H. *The Architecture of Complexity*. 457–476 (1991). doi:10.1007/978-1-4899-0718-9\_31
42. Fodor, J. A. *The Mind Doesn’t Work that Way*. (MIT Press, 0).
43. Coltheart, M. Modularity and cognition. *Trends in Cognitive Sciences* **3**, 115–120
44. Robinson, Henderson, Matar, Riley & Gray. Dynamical reconnection and stability constraints on cortical network architecture. *Physical review letters* **103**, 108104 (2009).
45. Clune, J., Mouret, J.-B. & Lipson, H. The evolutionary origins of modularity. *Proceedings of the Royal Society B: Biological Sciences* **280**, 20122863 (2013).
46. Tosh, CR & McNally, L. The relative efficiency of modular and non-modular networks of different size. *Proceedings of the Royal Society B: Biological Sciences* **282**, 20142568–20142568
47. Stevens, A., Tappon, S., Garg, A. & Fair, D. Functional brain network modularity captures inter- and intra-individual variation in working memory capacity. *PloS one* **7**, e30468 (2012).
48. Arnemann, K. *et al.* Functional brain network modularity predicts response to cognitive training after brain injury. *Neurology* **84**, 1568–74 (2015).
49. Gollo, L., Zalesky, A., Hutchison, van den Heuvel, M. & Breakspear, M. Dwelling quietly in the rich club: brain network determinants of slow cortical fluctuations. *Philosophical transactions of the Royal Society of London. Series B, Biological sciences* **370**, (2015).
50. Margulies, D. *et al.* Situating the default-mode network along a principal gradient of macroscale cortical organization. *Proceedings of the National Academy of Sciences of the United States of America* **113**, 12574–12579 (2016).
51. Nguyen, J. P. *et al.* Whole-brain calcium imaging with cellular resolution in freely behaving *Caenorhabditis elegans*. *Proceedings of the National Academy of Sciences* **113**, E1074–E1081 (2016).
52. White, Southgate, Thomson & Brenner. The Structure of the Nervous System of the Nematode *Caenorhabditis elegans*. *Philosophical Transactions of the Royal Society B: Biological Sciences* **314**, 1–340 (1986).
53. Essen, D. *et al.* The WU-Minn Human Connectome Project: an overview. *NeuroImage* **80**, 62–79 (2013).
54. Cox. AFNI: software for analysis and visualization of functional magnetic resonance neuroimages. *Computers and biomedical research, an international journal* 162–73 (1996). doi:10.1006/cbmr.1996.0014
55. Young, M. P. The organization of neural systems in the primate cerebral cortex. *Proceedings. Biological sciences* **252**, 13–18 (1993).

## Extended Data Figures



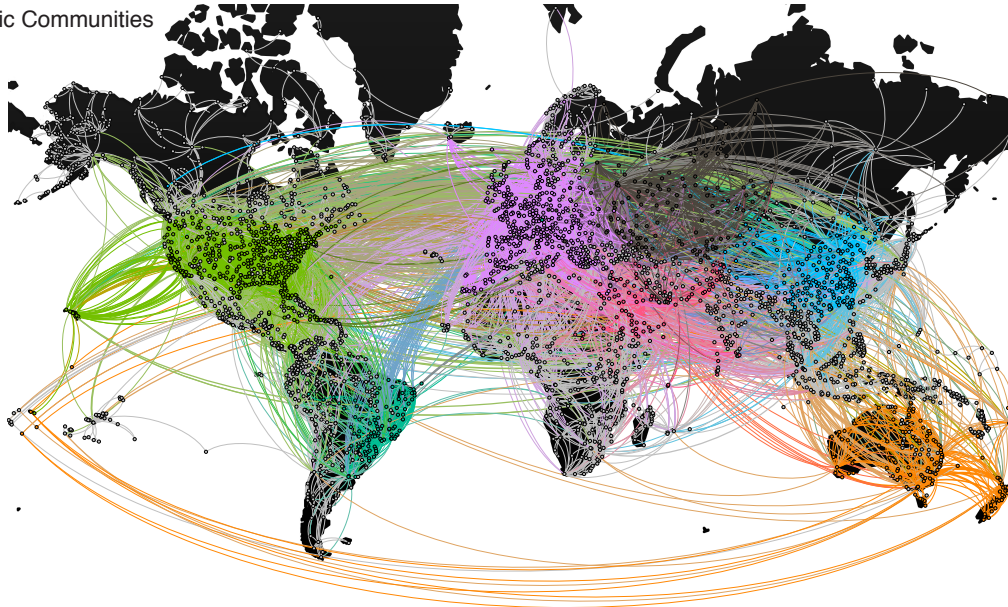
**Extended Data Figure 1 | Clubness of the four *c elegans* functional networks.** **a**, Normalized club coefficients are calculated with random graphs that place the edges randomly, but retain each node's degree and sum of weights, which accounts for the contribution of edge placement, but not edge weights, to the normalized club coefficient. **b**, Normalized club coefficients are calculated with random graphs, where all nodes maintain their degree, but the edges are randomly placed and the edge weights are shuffled between nodes with the same degree, which accounts for the contribution of both edge placement and edge weights to the normalized club coefficient. This latter method is the method reported in Figure 1.



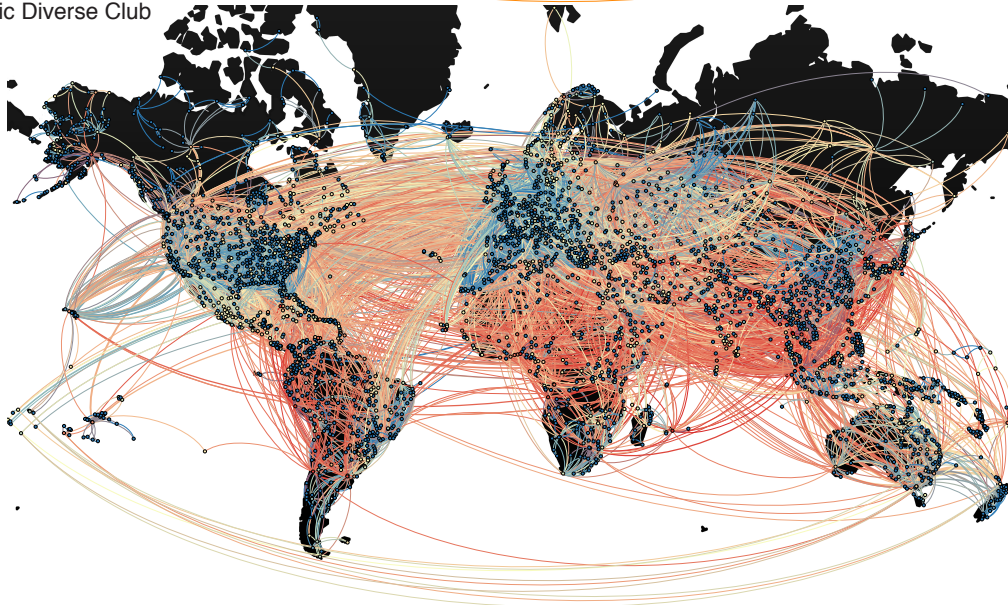


**Extended Data Figure 2 | Clubness of the human functional networks and the air traffic network.** Normalized club coefficients are calculated with random graphs that place the edges randomly, but retain each node's degree and sum of weights, which accounts for the contribution of edge placement, but not edge weights, to the normalized club coefficient.

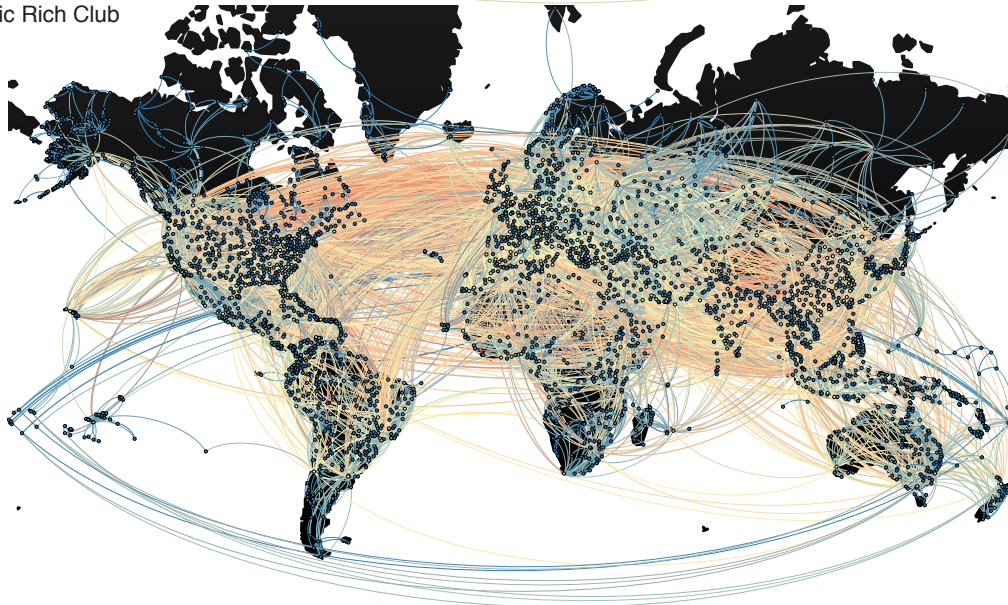
Air Traffic Communities



Air Traffic Diverse Club

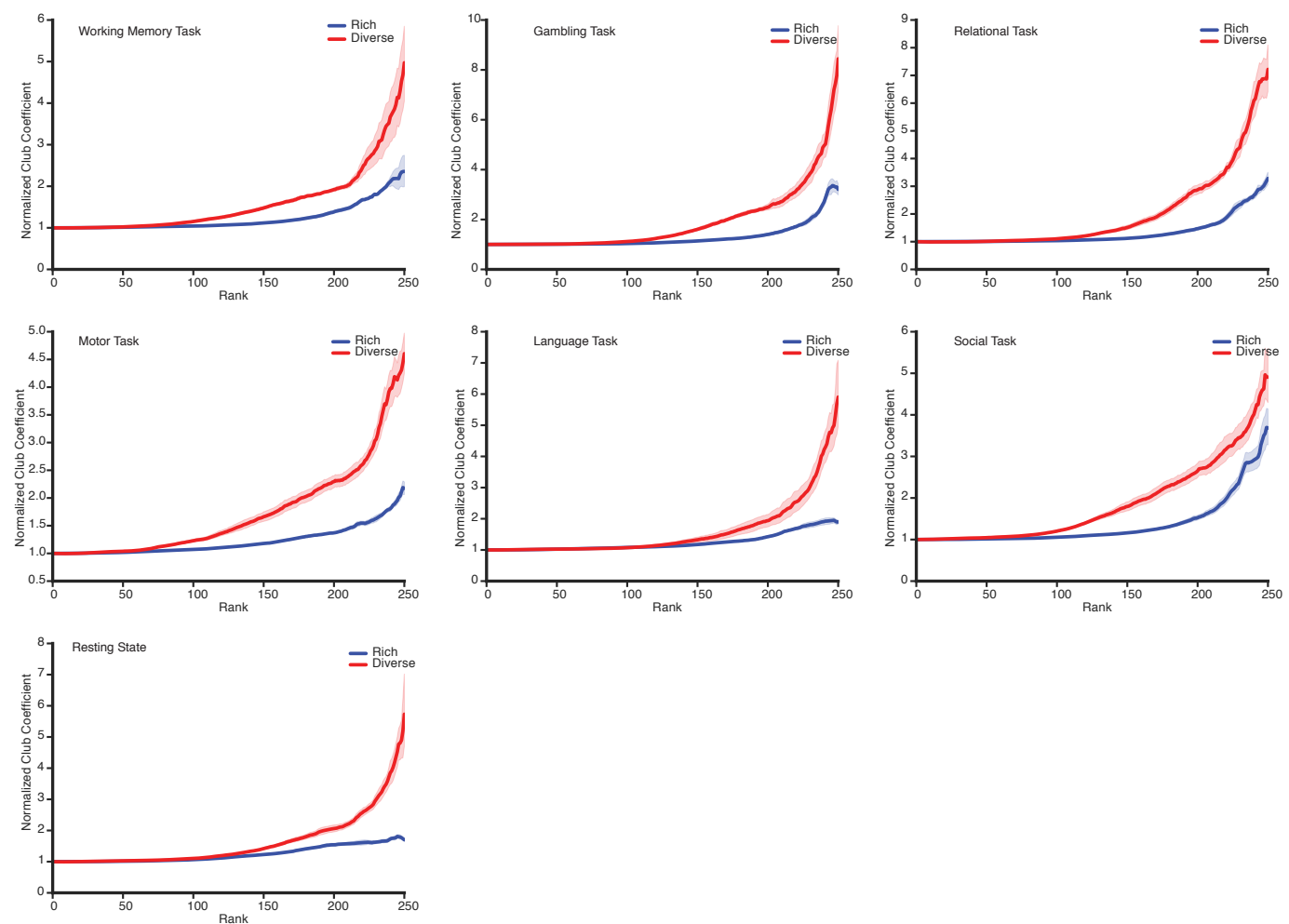


Air Traffic Rich Club

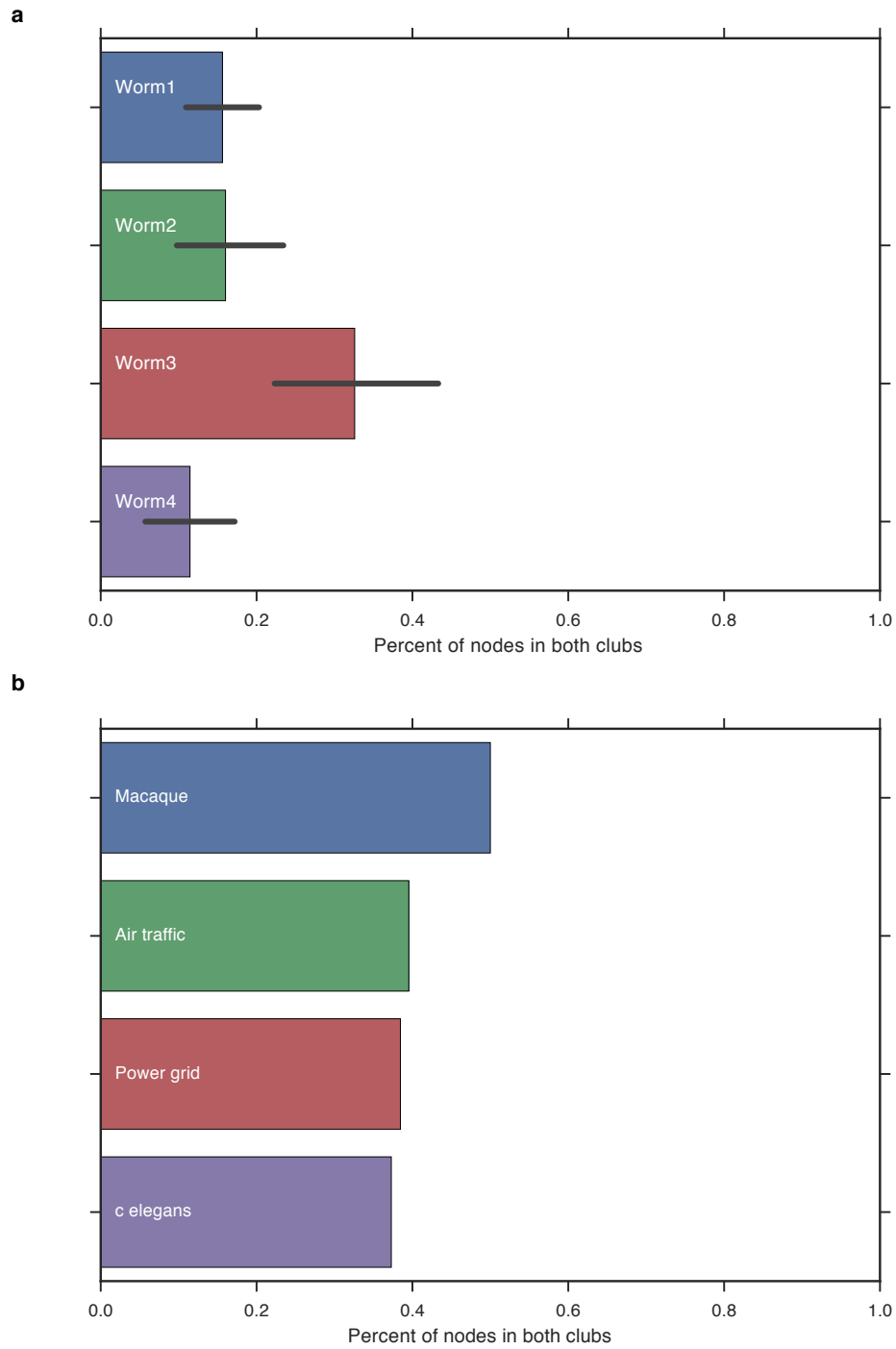


**Extended Data Figure 3 | Air traffic communities and clubs.** Top, community detection results from the air traffic network. Here, each node is colored according to the community it is in. Middle, diverse club; bottom, rich club. Nodes in

red represent the maximum value for the given metric (participation coefficient or degree), yellow is median, and blue is the minimum. Edges are colored by the mix between the two nodes each edge connects. Edges represent a flight route, with red edges being intra club, yellow between a club node and a non-club node, and blue as between two non-club nodes. Note that, only in the diverse club, non-club flights are predominately domestic, with diverse club flights predominately being international. This is in line with our finding that the airports with the highest participation coefficients are all international airports.

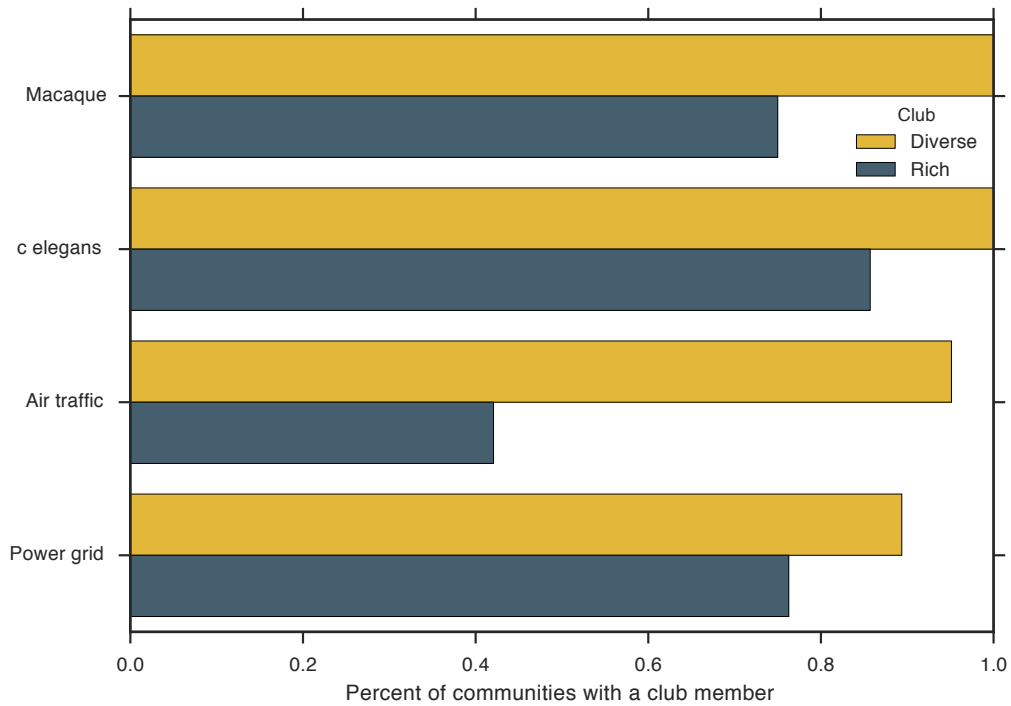


**Extended Data Figure 4 | Clubness for all 7 human functional network states.** Normalized club coefficients are calculated with random graphs, where all nodes maintain their degree, but the edges are randomly placed and the edge weights are shuffled between nodes with the same degree, which accounts for the contribution of both edge placement and edge weights to the normalized club coefficient. Shaded regions represent 95% confidence intervals across costs.

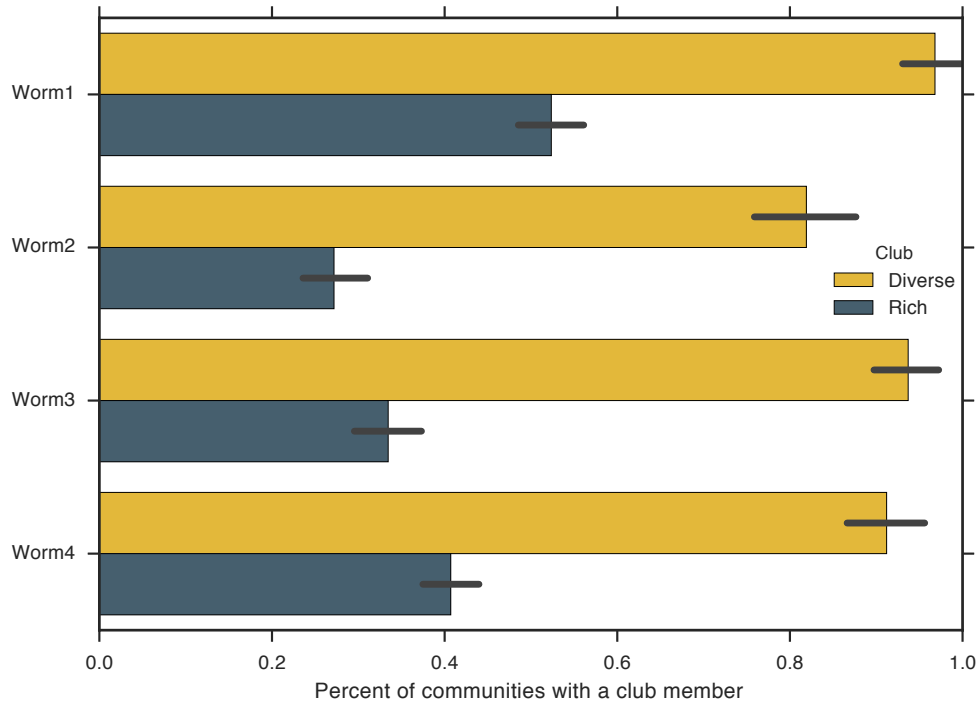


**Extended Data Figure 5 | Overlapping members of the clubs.** Percentage of nodes that are in both clubs for the four *c. elegans* functional networks (mean across costs) and structural networks. Zero percent represents that no nodes were members of both clubs, and 100 percent represents that the clubs are identical.

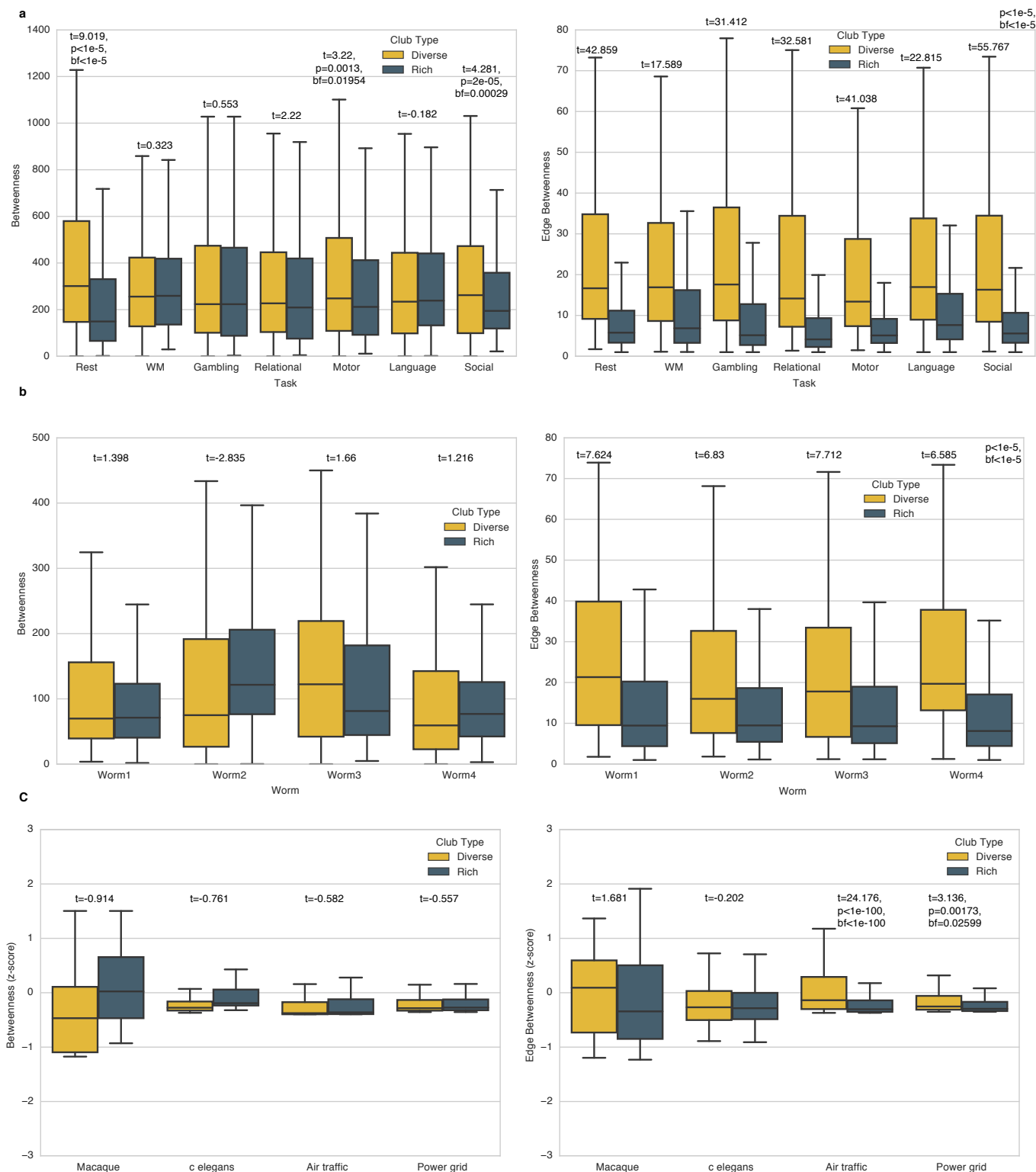
**a**



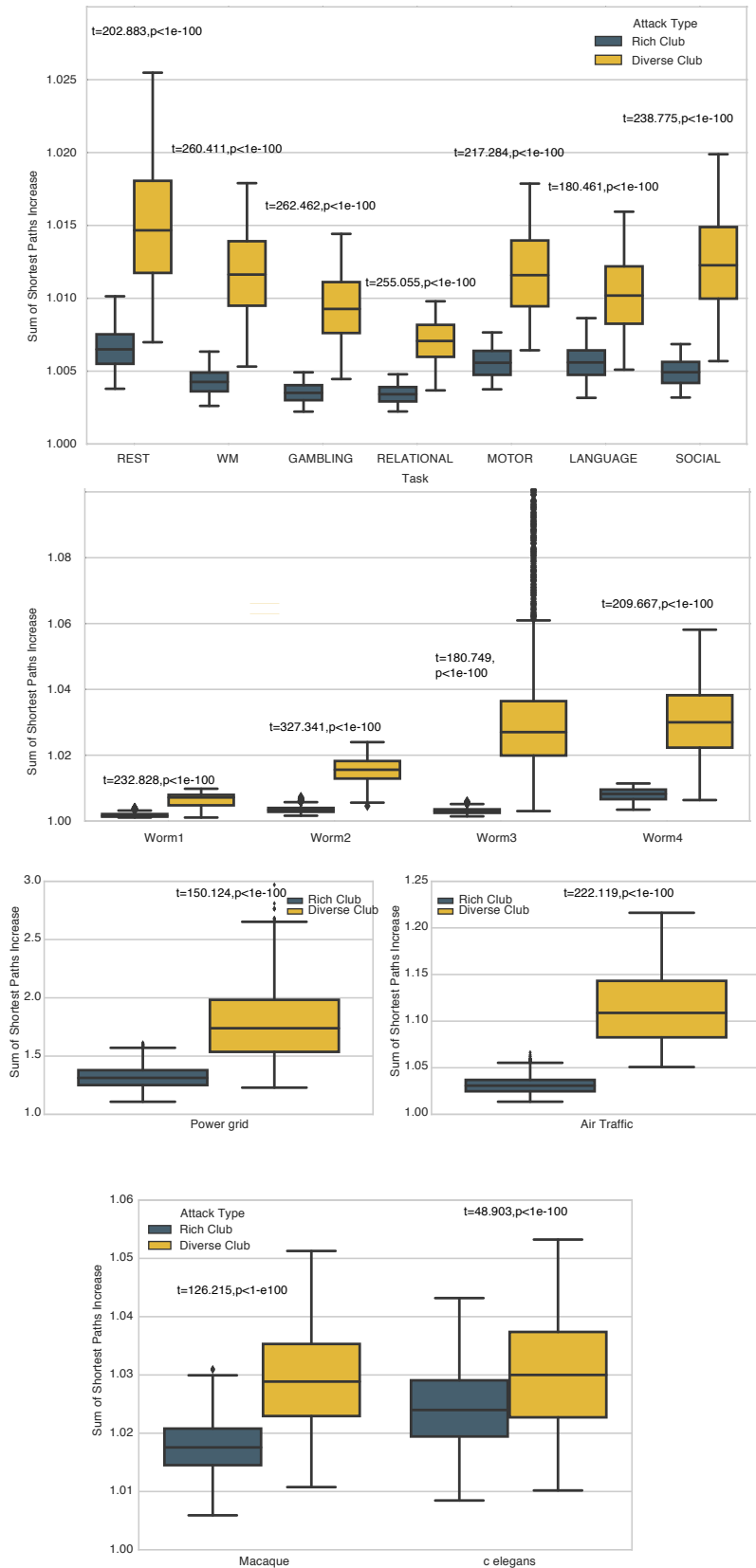
**b**



**Extended Data Figure 6 | Distribution of clubs' members across communities.** For each network, the percentage of communities with a node from the rich club and the diverse club is plotted. 100 percent represents that every community contains at least one node from that club. **a**, structural networks. **b**, functional networks from four *c. elegans* worms.

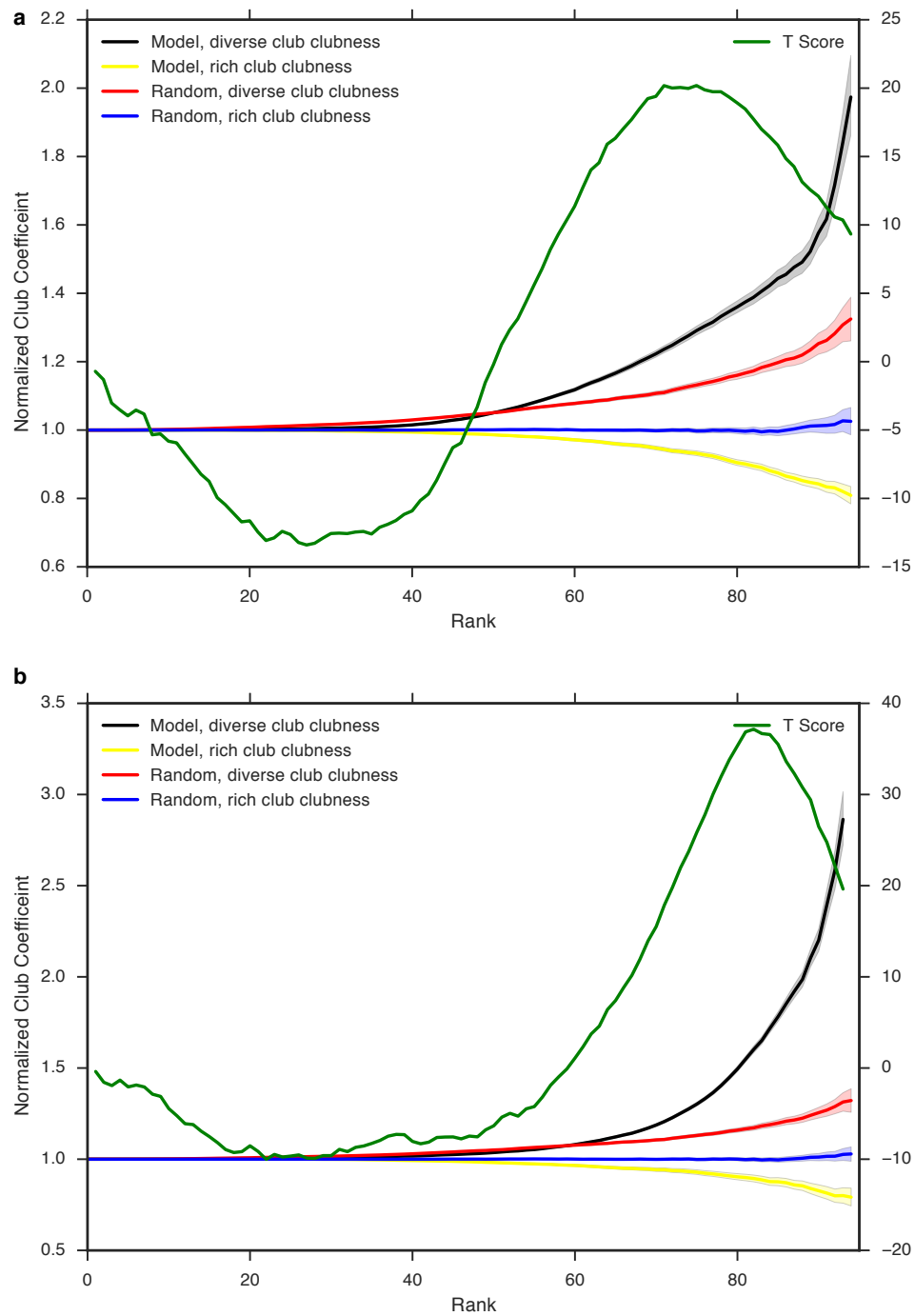


**Extended Data Figure 7 | Distribution of betweenness centrality and edge centrality scores.** Betweenness centrality measures how many shortest paths cross through a particular node, while edge betweenness measures how many shortest paths cross a particular edge. Only edges between club members were included in the calculation for edge betweenness. A significant Bonferroni ( $bf$ , number of tests=15) corrected  $p$  value is shown if the result was significant for that particular network. Pooling betweenness across costs and tasks for the human networks, the diverse club was significantly higher in betweenness than the rich club ( $t=7.2$ , Bonferroni,  $p=2.9e-14$ ). Pooling betweenness across costs and worms for the *c. elegans* networks, there was no significant difference ( $t=0.35$ ). Pooling betweenness across structural networks, there was also no significant difference ( $t=-0.6$ ). In all networks besides the structural macaque and *c. elegans* the edge betweenness of the diverse club was significantly higher than that of the rich club.



**Extended Data Figure 8 | Targeted Attacks.** Sum of shortest paths after attacks on the rich club or the diverse club for every network. For each network, over 10,000 iterations, we removed anywhere (randomly) between 50 and 90 percent of edges (skipping edges that disconnected the graph into two sub-graphs) from the rich club or the diverse club. We then calculated the increase in the sum of shortest paths. An increase in the sum of shortest paths indicates decreased global efficiency.





**Extended Data Figure 9 | Generative Models.** Alternative ratios of  $Q$  to efficiency for the generative models (0.70(a), and 0.80(b)).

Acknowledgments. M.A.B and M.D. are supported by NIH Grant NS79698 and the National Science Foundation Graduate Research Fellowship Program under Grant no. DGE1106400. B.T.T.Y. is supported by Singapore MOE Tier 2 (MOE2014-T2-2-016), NUS Strategic Research (DPRT/944/09/14), NUS SOM Aspiration Fund (R185000271720), Singapore NMRC (CBRG14nov007, NMRC/CG/013/2013) and NUS YIA.

Author contributions. M.A.B. devised the concept and study; M.A.B., B.T.T.Y., and M.D. jointly designed the analyses; M.A.B. contributed new reagents/analytic tools; M.A.B. ran the experiments and analyzed the data; M.A.B., B.T.T.Y., and M.D. wrote the paper.

Author Affiliations. M.A.B and M.D., Helen Willis Neuroscience Institute & Department of Psychology, University of California, Berkeley, California, USA. B.T.T.Y. Electrical and Computer Engineering, Clinical Imaging Research Centre, Singapore Institute for Neurotechnology & Memory Networks Programme, National University of Singapore, Singapore.